Density functional theory for nearest-neighbor exclusion lattice gases in two and three dimensions

Luis Lafuente* and José A. Cuesta†
Grupo Interdisciplinar de Sistemas Complejos (GISC), Departamento de Matemáticas, Universidad Carlos III de Madrid, Avenida de la Universidad 30, 28911 Leganés, Madrid, Spain
(Received 13 August 2003; published 30 December 2003)

To speak about fundamental measure theory obliges us to mention dimensional crossover. This feature, inherent to the systems themselves, was incorporated in the theory almost from the beginning. Although at first it was thought to be a consistency check for the theory, it rapidly became its fundamental pillar, thus becoming the only density functional theory which possesses such a property. It is straightforward that dimensional crossover connects, for instance, the parallel hard cube system (three dimensional) with that of squares (two dimensional) and rods (one dimensional). We show here that there are many more connections which can be established in this way. Through them we deduce from the functional for parallel hard (hyper)cubes in the simple (hyper)cubic lattice the corresponding functionals for the nearest-neighbor exclusion lattice gases in the square, triangular, simple cubic, face-centered-cubic, and body-centered-cubic lattices. As an application, the bulk phase diagram for all these systems is obtained.

DOI: 10.1103/PhysRevE.68.066120 PACS number(s): 05.50.+q, 64.60.Cn, 61.20.Gy, 05.20.Jj

I. INTRODUCTION

Rosenfeld's fundamental measure (FM) theory [1] is peculiar among the weighted density approximations (WDAs), and it is so for many reasons. To begin with, classical WDAs are constructed upon the knowledge of the thermodynamics and structure of the uniform fluid, while FM theory is constructed on a geometrical basis. Originally it needed scaled-particle theory to produce a functional, but in its latest formulations this is not a requirement anymore [2,3], and geometry stands as its unique ingredient. Another important difference is that, while the extension to mixtures of classical WDAs is far from being straightforward, the natural formulation of FM theory is for a mixture (although it has recently been shown that a FM theory for hard spheres does not accommodate a description for mixtures as well as it was previously thought [4]). One further remarkable feature is that FM theory performs best where classical theories are poorest: in the high density region. It has been shown, for instance, that the description FM theory provides for a solid is extraordinarily accurate in all its details [3,5]. This is probably the reason why the belief has spread that FM theory is the best density functional theory for the system of hard spheres. But there is no free lunch. Such a peculiar structure makes the theory extremely rigid, so much that it is very difficult (sometimes impossible) to improve a particular detail without spoiling another. This shows up very clearly if one tries to improve the equation of state for the liquid phase. FM theory yields the scaled particle equation of state. The large difference in accuracy between the liquid and the solid gives rise to a not very good prediction of freezing [3]. If one tries to replace the equation of state by, e.g., Carnahan-Starling, the internal structure of the theory squeaks [6] and loses some of its nice features (although for some purposes the defects may be mostly irrelevant [7]).

But by far the most genuine property of FM theory is dimensional crossover, something that this theory shares with the exact functionals and with no other known density functional theory. In its first formulation this property was introduced as the ability of a modification of Rosenfeld's original functional for hard spheres to recover the exact functional for ''zero-dimensional'' cavities (cavities which cannot hold more than one sphere) [8], but it was immediately extended to describe the property of the exact d-dimensional functional to reproduce the exact $(d-1)$-dimensional one when evaluated at a density profile which is delta-like on a hyperplane [9]. Needless to say, functionals that have dimensional crossover are particularly suitable for studying fluids under strong confinement.

The first modified FM functional for hard spheres produced accurate functionals for $d=2$ and $d=1$, apart from yielding the exact one for $d=0$ (cavities) [9]. When applied to the system of parallel hard cubes, whose FM functional can be obtained for arbitrary dimension (being exact in $d=1$) [10], it was shown that dimensional crossover consistently transforms the d-dimensional functional into the $(d-1)$-dimensional one, down to $d=0$. The acknowledgment that this property lies at the heart of the formal theory suggested the last step in this direction: transforming this property into the constructive principle of FM theory [2,3]. Under this new formulation FM theory has been generalized to systems with soft interaction potentials [11], anisotropic hard-particle models [12,13], nonadditive mixtures [14], lattice gases [15–17], and even fluids in porous media [18,19].

So we see that dimensional crossover was first looked at as a very stringent constraint on density functionals and later as a way of rising from $d=0$ and $d=1$ to $d>1$ in the construction of FM functionals. But dimensional crossover has another use which has hardly been exploited: one can get new systems out of known ones. The first (and to our knowledge the only) example of such a use was already provided by Rosenfeld *et al.* [9]. By forcing hard spheres to have their centers of mass on one out of two parallel planes separated a distance shorter than a sphere diameter, one obtains a binary

*Electronic address: llafuent@math.uc3m.es
†Electronic address: cuesta@math.uc3m.es

mixture of nonadditive hard spheres with negative nonadditivity ($2\sigma_{12}<\sigma_{11}+\sigma_{22}$, with σ_{ij} the center-to-center contact distance between spheres of type i and j). The amount of nonadditivity depends on the distance between planes.

Physically, dimensional crossover amounts to applying an infinite-strength external potential all over a $(d+1)$-dimensional lattice, except in a certain d-dimensional set of sites which defines the effective system. But this is not the only way to construct functionals for new systems out of known ones. One can also apply an appropriate external potential at selected sites and modify the interaction accordingly, thus obtaining a new system without reducing dimension. This trick has already been applied to obtain the exact functional for a nonadditive mixture of hard rods in a one-dimensional lattice from that of the additive mixture [16].[1]

One can consider all systems which are related through the kind of transformations we have just described above. Then, because of the internal consistency the FM theory has, the functional for a given model ''contains'' the functional for any other model to which it is related. Our goal in this paper is to show how this works for a set of well-known lattice gases. The methods we will use are very general, so their application to other families of models should not be difficult. This is interesting if we take into account the importance that lattice gases are getting in the study of certain inhomogeneous problems, such as the behavior of fluids in porous media [19–21].

The paper is organized as follows. Section II describes the general procedure to obtain the excess free-energy functional for nearest-neighbor exclusion lattice gases in different lattices, either starting from a higher dimensional functional for cubes and using dimensional reduction to a plane or a hyperplane (this procedure is subsequently applied to the square, triangular, simple cubic, and face-centered-cubic lattices), or starting from the functional of cubes and applying an infinite-strength external potential in the appropriate set of lattice sites without reducing the effective dimensionality of the system (this procedure is the one applied for the body-centered-cubic lattice). The final (simple) expressions for the functionals are explicitly obtained in closed form. In Sec. III these functionals are applied to obtain the bulk phase diagram for all the systems considered. There, FM theory results are compared with those from other classical theories, showing that the former is at least at the same level of accuracy than the latter. Finally, we conclude in Sec. IV.

II. THEORY

In this section we will derive the FM functional for lattice gases with nearest-neighbor exclusion in five different lattices: square (hard-square lattice gas), triangular (hard-hexagon lattice gas), simple cubic (sc), faced-centered-cubic (fcc), and body-centered-cubic (bcc). All these systems have been already considered in the literature as simple models for the hard-sphere system [22]. As explained in the Introduction, the derivation of the first four will make use of the dimensional crossover property of FM functionals, so all the four will be obtained from the known functional for $(d+1)$-dimensional parallel hard cubes in a simple (hyper)cubic lattice [16,17] (d being the dimensionality of the final systems). For the last one, we will start from the functional for the three-dimensional parallel hard cubes in the simple cubic lattice, and we will apply an infinite-strength external potential to the appropriate set of lattice sites of the original lattice, so that the effective lattice becomes a bcc one. The fact that all the models considered exclude only nearest neighbors forces the edge length of the cubes to be $\sigma=2$ lattice spacings.

Of the different ways in which the FM functional for this particular model of (hyper)cubes can be written [16,17], the simplest expression for the excess free energy is probably

$$\beta\mathcal{F}_{\mathrm{ex}}[\rho]=\sum_{\mathbf{s}\in\mathbb{Z}^d}\sum_{\mathbf{k}\in\{0,1\}^d}(-1)^{d-k}\Phi_0(n^{(\mathbf{k})}(\mathbf{s})), \tag{1}$$

where $n^{(\mathbf{k})}(\mathbf{s})$ are the weighted densities

$$n^{(\mathbf{k})}(\mathbf{s})=\sum_{\mathbf{r}\in\mathcal{B}(\mathbf{k})}\rho(\mathbf{s}+\mathbf{r}) \tag{2}$$

labeled by the vector index $\mathbf{k}=(k_1,\ldots,k_d)$, $k=\Sigma_{l=1}^{d}k_l$, $\mathcal{B}(\mathbf{k})$ denotes the set

$$\mathcal{B}(\mathbf{k})=\{\mathbf{r}\in\{0,1\}^d:0\leqslant r_i\leqslant k_i,\ \ i=1,\ldots,d\} \tag{3}$$

and $\Phi_0(\eta)=\eta+(1-\eta)\ln(1-\eta)$ is the excess free energy for a zero-dimensional cavity with mean occupancy $0\leqslant\eta\leqslant1$ (β is the reciprocal temperature in Boltzmann's constant units).

A. Square lattice

The kind of dimensional reduction we have to perform in order to obtain the hard-square lattice gas out of cubes in a cubic lattice is illustrated in Fig. 1. It amounts to forcing the centers of mass of the cubes to lie in the plane

$$\mathcal{P}_{\mathrm{sq}}=\{(s_1,s_2,s_3)\in\mathbb{Z}^3:s_1+s_2+2s_3=0\}. \tag{4}$$

(Notice that we might have chosen several equivalent planes, given the symmetry of the system.) Figure 1 shows that the effective underlying lattice is a square lattice defined, for instance, by the pair of orthogonal vectors $\{\mathbf{e}_1=\mathbf{b}_2-\mathbf{b}_1,\ \mathbf{e}_2=\mathbf{b}_3-\mathbf{b}_1-\mathbf{b}_2\}$ of the plane $\mathcal{P}_{\mathrm{sq}}$, $\{\mathbf{b}_1,\mathbf{b}_2,\mathbf{b}_3\}$ being the canonical vector basis in $\mathbb{Z}^3$. Furthermore, the effective interaction potential between the cubes within this lattice is nearest-neighbor exclusion.

In terms of the one-particle distribution function, the dimensional reduction can be imposed by setting

$$\rho(\mathbf{s})=\rho(s_2+s_3,s_3)\,\delta(s_1+s_2+2s_3), \tag{5}$$

[1] A similar trick can be employed to recover the exact functional for the one-dimensional system of hard rods in a lattice (see Ref. [16]) from the exact functional of its continuum counterpart [42], by inserting in the latter a density profile formed by a chain of delta spikes [43].

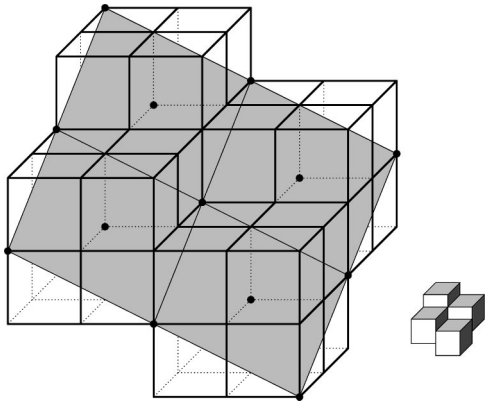

FIG. 1. Hard cubes with edge length $\sigma=2$ in a simple cubic lattice. Their centers of mass are constrained to lie on the plane $s_1+s_2+2s_3=0$. Filled circles mark the sites excluded by the cubes which lie on this plane. Notice that on the plane, cubes behave as the hard-square lattice gas with nearest-neighbor exclusion. The diagram at the lower right corner helps us to visualize the relative position of the cubes in the figure.

where $\delta(0)=1$ and $\delta(x\neq 0)=0$ (a Kronecker symbol). The dependence of the two-dimensional density profile reflects the choice of basis vectors.

To obtain the FM functional for the hard-square lattice gas it only remains to introduce the density profile (5) in the functional (1) through the weighted densities (2) and to eliminate the unnecessary degrees of freedom. In what follows, we will carry out this task in detail.

The contribution of one weighted density, say $n^{(\mathbf{k})}(\mathrm{s})$, to the excess free-energy functional will be [up to the sign $(-1)^{d-k}$]

$$\sum_{\mathbf{s}\in\mathbb{Z}^3}\Phi_0\left(\sum_{\mathbf{r}\in\mathcal{B}(\mathbf{k})}\rho(s_2+r_2+r_3,s_3+r_3)\,\delta(s_1+u)\right),$$

where $u\equiv r_1+r_2+2r_3$ and we have made use of the translational invariance in **s**. A better way of expressing this is to split the sum in **r** according to the values of u, as

$$\sum_{\mathbf{s}\in\mathbb{Z}^3}\Phi_0\left(\sum_{u=0}^{4}\delta(s_1+u)\sum_{(\mathbf{r}|u,\mathbf{k})}\rho(s_2+r_2+r_3,s_3+r_3)\right),$$

where $(\mathbf{r}|u,\mathbf{k})$ denotes those vectors $\mathbf{r}\in\mathcal{B}(\mathbf{k})$ which verify $r_1+r_2+2r_3=u$. Now, one and only one of the δ functions within the sum in **r** is 1; the others are 0, so the above expression admits the following rewriting:

$$\sum_{\mathbf{s}\in\mathbb{Z}^3}\sum_{u=0}^{4}\delta(s_1+u)\Phi_0\left(\sum_{(\mathbf{r}|u,\mathbf{k})}\rho(s_2+r_2+r_3,s_3+r_3)\right).$$

The sum over s_1 is now trivial, so denoting $\mathbf{t}\equiv(s_2,s_3)$, the expression simplifies to

TABLE I. Coefficients of the linear combinations $\Sigma_l a_l(\mathbf{k})\rho(\mathbf{t}+\mathbf{e}_l)$ appearing in Eq. (6), which define the weighted densities for the hard-square lattice gas model.

u	$a_0(\mathbf{k})$	$a_1(\mathbf{k})$	$a_2(\mathbf{k})$
0	1	0	0
1	k_1	k_2	0
2	k_1k_2	0	k_3
3	k_1k_3	k_2k_3	0
4	$k_1k_2k_3$	0	0

$$\sum_{\mathbf{t}\in\mathbb{Z}^2}\sum_{u=0}^{4}\Phi_0\left(\sum_{(\mathbf{r}|u,\mathbf{k})}\rho(s_2+r_2+r_3,s_3+r_3)\right).$$

The last step concerns the identification of the argument of Φ_0 (the new measures for the effective system). Using the translational invariant in **t** the above expression can always be written

$$\sum_{\mathbf{t}\in\mathbb{Z}^2}\sum_{u=0}^{4}\Phi_0\left(\sum_{l=0}^{2}a_l(\mathbf{k})\rho(\mathbf{t}+\mathbf{e}_l)\right), \tag{6}$$

where $\mathbf{e}_0=(0,0)$, $\mathbf{e}_1=(1,0)$, and $\mathbf{e}_2=(0,1)$, and the coefficients $a_l(\mathbf{k})$ are listed in Table I [notice that $\Phi_0(0)=0$, so for some u and **k** there will be no contribution].

It is now time to reinsert Eq. (6) back into Eq. (1), group terms, and write the final form for the functional,

$$\beta\mathcal{F}_{\mathrm{ex}}^{\mathrm{sq}}[\rho]=\sum_{\mathbf{s}\in\mathbb{Z}^2}[\Phi_0[\rho(\mathbf{s})+\rho(\mathbf{s}+\mathbf{e}_1)]+\Phi_0[\rho(\mathbf{s})+\rho(\mathbf{s}+\mathbf{e}_2)]-3\Phi_0(\rho(\mathbf{s}))]. \tag{7}$$

The above expression can be more easily visualized by using the diagrammatic notation introduced in [17],

$$\beta\mathcal{F}_{\mathrm{ex}}^{\mathrm{sq}}[\rho]=\sum_{\mathbf{s}\in\mathbb{Z}^2}[\Phi_0(\circ\!-\!\circ)+\Phi_0\left(\begin{smallmatrix}\circ\\ \circ\end{smallmatrix}\right)-3\Phi_0(\circ)]. \tag{8}$$

Its meaning should be clear by comparing Eqs. (7) and (8).

B. Triangular lattice

As in the preceding section, we will start with the FM functional for the parallel hard cubes with $\sigma=2$ in the simple cubic lattice. As the procedure we will follow is the same as the one used before, we will omit most details. Again, we will restrict the position of the centers of mass of the cubes to lie, in this case, in the plane

$$\mathcal{P}_{\mathrm{tr}}=\{(s_1,s_2,s_3)\in\mathbb{Z}^3:s_1+s_2+s_3=0\}. \tag{9}$$

A sketch of the effect of this confinement is shown in Fig. 2. It can be appreciated that the resulting effective lattice is a triangular lattice, and that the interaction becomes again nearest-neighbor exclusion. The effective system thus corresponds to the hard-hexagon lattice gas.

The one-particle distribution function for this confined system can be written

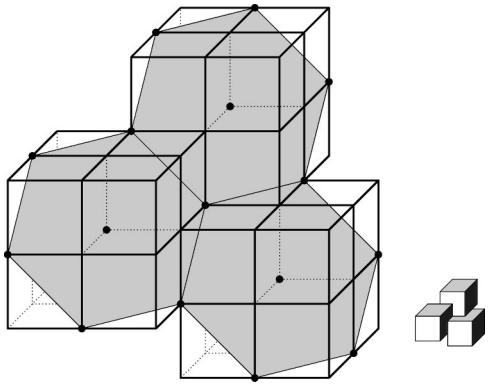

FIG. 2. Hard cubes with edge length $\sigma=2$ in a simple cubic lattice. Their centers of mass are constrained to lie on the plane $s_1+s_2+s_3=0$. Filled circles mark the sites excluded by the cubes which lie on this plane. Notice that on the plane, cubes behave as the hard-hexagon lattice gas with nearest-neighbor exclusion. The diagram at the lower right corner helps us to visualize the relative position of the cubes in the figure.

$$\rho(s_1,s_2,s_3)=\rho(s_2,s_3)\,\delta(s_1+s_2+s_3), \tag{10}$$

where the arguments of the two-dimensional density profile correspond to the choice $\{\mathbf{e}_1=\mathbf{b}_2-\mathbf{b}_1,\ \mathbf{e}_2=\mathbf{b}_3-\mathbf{b}_1\}$ for a vector basis.

After eliminating the unnecessary degrees of freedom, the resulting contribution of $n^{(\mathbf{k})}(\mathbf{s})$ to the excess free-energy functional is

$$\sum_{\mathbf{t}\in\mathbb{Z}^2}\sum_{u=0}^{3}\Phi_0\left(\sum_{(\mathbf{r}|u,\mathbf{k})}\rho(t_1+r_2,t_2+r_3)\right), \tag{11}$$

using the same notation as in the previous case. Now $u\equiv r_1+r_2+r_3$. This can again be written

$$\sum_{\mathbf{t}\in\mathbb{Z}^2}\sum_{u=0}^{3}\Phi_0\left(\sum_{l=0}^{3}a_l(\mathbf{k})\rho(\mathbf{t}+\mathbf{e}_l)\right), \tag{12}$$

where the coefficients $a_l(\mathbf{k})$ appear in Table II (a third vector, $\mathbf{e}_3=\mathbf{e}_2-\mathbf{e}_1$, is involved this time).

Inserting this in Eq. (1) and regrouping terms, the excess free-energy functional for the hard-hexagon model turns out to be

TABLE II. The same as Table I for the linear combinations in Eq. (12) defining the weighted densities for the hard-hexagon lattice gas model.

u	$a_0(\mathbf{k})$	$a_1(\mathbf{k})$	$a_2(\mathbf{k})$	$a_3(\mathbf{k})$
0	1	0	0	0
1	k_1	k_2	k_3	0
2	0	k_1k_2	k_1k_3	k_2k_3
3	$k_1k_2k_3$	0	0	0

$$\beta\mathcal{F}_{\mathrm{ex}}^{\mathrm{tr}}[\rho]=\sum_{\mathbf{s}\in\mathbb{Z}^2}\Big[\Phi_0(n^{(+)}(\mathbf{s}))+\Phi_0(n^{(-)}(\mathbf{s}))-\sum_{l=1}^{3}\Phi_0(n^{(l)}(\mathbf{s}))+\Phi_0(\rho(\mathbf{s}))\Big], \tag{13}$$

where we have defined the new set of weighted densities

$$n^{(\pm)}(\mathbf{s})=\rho(\mathbf{s})+\rho(\mathbf{s}\pm\mathbf{e}_1)+\rho(\mathbf{s}\pm\mathbf{e}_2),$$

$$n^{(l)}(\mathbf{s})=\rho(\mathbf{s})+\rho(\mathbf{s}+\mathbf{e}_l),\quad l=1,2,3. \tag{14}$$

In diagrammatic notation,

$$\beta\mathcal{F}_{\mathrm{ex}}^{\mathrm{tr}}[\rho]=\sum_{\mathbf{s}\in\mathbb{Z}^2}[\Phi_0(\ )+\Phi_0(\ )-\Phi_0(\ )-\Phi_0(\ )-\Phi_0(\ )+\Phi_0(\ )]. \tag{15}$$

C. Simple cubic lattice

As in the two preceding systems, we will write down a closed-form free-energy density functional for this model, but now we have to start from a four-dimensional system of $\sigma=2$ parallel hypercubes in a simple hypercubic lattice and constrain the centers of mass of the hypercubes to be in the three-dimensional hyperplane

$$\mathcal{P}_{\mathrm{sc}}\equiv\{(s_1,s_2,s_3,s_4)\in\mathbb{Z}^4: s_1+s_2+2s_3+4s_4=0\}. \tag{16}$$

As this cannot be graphically sketched we should clarify why we chose this particular hyperplane. A hypercube with $\sigma=2$ centered at the origin contains all lattice sites $\mathbf{s}$ with coordinates $s_l=0,\ \pm1,\ l=1,...,4$. Now, the intersection of such a hypercube with $\mathcal{P}_{\mathrm{sc}}$ can be split into two sets: one with $s_4=0$ and $s_1+s_2+2s_3=0$, and the other one with $s_4=\pm1$ and $s_1+s_2+2s_3=\mp4$. These two sets define three parallel (three-dimensional) planes. The first one coincides with $\mathcal{P}_{\mathrm{sq}}$, Eq. (4) (hence the choice of the coefficients of these three coordinates in $\mathcal{P}_{\mathrm{sc}}$) and thus includes the five points (including the origin) of the two-dimensional square lattice of Sec. II A. The last two planes contain only one site each (symmetrically placed with respect to the origin). Excluding the origin, these sites complete the six vertices of the octahedron defining the "shape" of the particle.

The effective underlying lattice is expanded, e.g., by the vector basis of the hyperplane $\{\mathbf{e}_1=\mathbf{b}_2-\mathbf{b}_1,\ \mathbf{e}_2=\mathbf{b}_3-\mathbf{b}_1-\mathbf{b}_2,\ \mathbf{e}_3=\mathbf{b}_4-\mathbf{b}_1-\mathbf{b}_2-\mathbf{b}_3\}$, with $\{\mathbf{b}_1,\mathbf{b}_2,\mathbf{b}_3,\mathbf{b}_4\}$ the canonical vector basis of $\mathbb{Z}^4$. Thus, the one-particle distribution function for this system can be written as

$$\rho(\mathbf{s})=\rho(s_2+s_3+2s_4,s_3+s_4,s_4)\,\delta(s_1+s_2+2s_3+4s_4), \tag{17}$$

where, again, the three-dimensional density profile corresponds to that of the effective system.

TABLE III. The same as Table I for the linear combinations in Eq. (18) defining the weighted densities for the nearest-neighbor exclusion lattice gas in the sc lattice.

u	$a_0(\mathbf{k})$	$a_1(\mathbf{k})$	$a_2(\mathbf{k})$	$a_3(\mathbf{k})$
0	1	0	0	0
1	k_1	k_2	0	0
2	k_1k_2	0	k_3	0
3	k_1k_3	k_2k_3	0	0
4	$k_1k_2k_3$	0	0	k_4
5	k_1k_4	k_2k_4	0	0
6	$k_1k_2k_4$	0	k_3k_4	0
7	$k_1k_3k_4$	$k_2k_3k_4$	0	0
8	$k_1k_2k_3k_4$	0	0	0

Repeating the procedure described in the previous examples we arrive at this expression for the contribution of $n^{(\mathbf{k})}(\mathbf{s})$ to the excess free-energy functional,

$$\sum_{\mathbf{t}\in\mathbb{Z}^3}\sum_{u=0}^{8}\Phi_0\left(\sum_{(\mathbf{r}|u,\mathbf{k})}\rho(t_1+v,t_2+r_3+r_4,t_3+r_4)\right),$$

where now $u\equiv r_1+r_2+2r_3+4r_4$ and v is a shorthand for $r_2+r_3+2r_4$. As in the preceding cases, this becomes

$$\sum_{\mathbf{t}\in\mathbb{Z}^3}\sum_{u=0}^{8}\Phi_0\left(\sum_{l=0}^{3}a_l(\mathbf{k})\rho(\mathbf{t}+\mathbf{e}_l)\right), \tag{18}$$

with $\mathbf{e}_0=(0,0,0)$, $\mathbf{e}_1=(1,0,0)$, $\mathbf{e}_2=(0,1,0)$, and $\mathbf{e}_3=(0,0,1)$, and the coefficients $a_l(\mathbf{k})$ given in Table III.

The final expression for the excess free-energy density functional of this model is

$$\beta\mathcal{F}_{\mathrm{ex}}^{\mathrm{sc}}[\rho]=\sum_{\mathbf{s}\in\mathbb{Z}^3}\left[\sum_{l=1}^{3}\Phi_0(n^{(l)}(\mathbf{s}))-5\Phi_0(\rho(\mathbf{s}))\right], \tag{19}$$

where $n^{(l)}(\mathbf{s})=\rho(\mathbf{s})+\rho(\mathbf{s}+\mathbf{e}_l)$, or diagrammatically,

$$\beta\mathcal{F}_{\mathrm{ex}}^{\mathrm{sc}}[\rho]=\sum_{\mathbf{s}\in\mathbb{Z}^3}[\Phi_0(\ \circ\atop\circ\ )+\Phi_0(\circ\!-\!\circ)+\Phi_0(\circ\!\!\circ)-5\Phi_0(\circ)]. \tag{20}$$

D. Face-centered-cubic lattice

The nearest-neighbor exclusion lattice gas in the fcc lattice can be obtained from the same four-dimensional system we have used above, but now the centers of mass of the hypercubes are confined to the three-dimensional hyperplane

$$\mathcal{P}_{\mathrm{fcc}}\equiv\{(s_1,s_2,s_3,s_4)\in\mathbb{Z}^4: s_1+s_2+s_3+2s_4=0\}. \tag{21}$$

A vector basis expanding the effective underlying three-dimensional fcc lattice is $\{\mathbf{e}_1=\mathbf{b}_2-\mathbf{b}_1,\ \mathbf{e}_2=\mathbf{b}_2-\mathbf{b}_3,\ \mathbf{e}_3=\mathbf{b}_4-\mathbf{b}_1-\mathbf{b}_3\}$. When a $\sigma=2$ hypercube is placed at the origin (0,0,0,0) the excluded sites in $\mathcal{P}_{\mathrm{fcc}}$ correspond to the set of 12 nearest neighbors of the fcc lattice, whose coordinates in the chosen basis are $\{\mathbf{e}_1=(1,0,0),\ \mathbf{e}_2=(0,1,0),\ \mathbf{e}_3=(0,0,1),\ \mathbf{e}_4=(1,-1,0),\ \mathbf{e}_5=(1,0,-1),\ \mathbf{e}_6=(0,1,-1)\}$ and the opposite ones. Under this external potential the one-particle distribution function takes the form

$$\rho(\mathbf{s})=\rho(s_2+s_3+s_4,-s_3-s_4,s_4)\,\delta(s_1+s_2+s_3+2s_4), \tag{22}$$

where the density profile in the right-hand side (rhs) is expressed in the chosen basis.

Proceeding as in the previous cases, the contribution of the weighted density $n^{(\mathbf{k})}(\mathbf{s})$ to the excess free-energy functional reads

$$\sum_{\mathbf{t}\in\mathbb{Z}^3}\sum_{u=0}^{5}\Phi_0\left(\sum_{(\mathbf{r}|u,\mathbf{k})}\rho(t_1+v,t_2-r_3-r_4,t_3+r_4)\right),$$

where now $u\equiv r_1+r_2+r_3+2r_4$ and v is a shorthand for $r_2+r_3+r_4$. This is more conveniently rewritten

$$\sum_{\mathbf{t}\in\mathbb{Z}^3}\sum_{u=0}^{5}\Phi_0\left(\sum_{l=0}^{5}a_l(\mathbf{k})\rho(\mathbf{t}+\mathbf{e}_l)\right), \tag{23}$$

with the coefficients $a_l(\mathbf{k})$ given in Table IV.

Gathering together the contributions of all weighted densities, as prescribed in Eq. (1), the excess free-energy density functional of this model turns out to be

$$\beta\mathcal{F}_{\mathrm{ex}}^{\mathrm{fcc}}[\rho]=\sum_{\mathbf{s}\in\mathbb{Z}^3}\left[\Phi_0(n^{(+)}(\mathbf{s}))+\Phi_0(n^{(-)}(\mathbf{s}))-\sum_{l=1}^{6}\Phi_0(n^{(l)}(\mathbf{s}))+5\Phi_0(\rho(\mathbf{s}))\right], \tag{24}$$

TABLE IV. The same as Table I for the linear combinations in Eq. (23) defining the weighted densities for the nearest-neighbor exclusion lattice gas in the fcc lattice.

u	$a_0(\mathbf{k})$	$a_1(\mathbf{k})$	$a_2(\mathbf{k})$	$a_3(\mathbf{k})$	$a_4(\mathbf{k})$	$a_5(\mathbf{k})$
0	1	0	0	0	0	0
1	k_1	k_2	0	0	k_3	0
2	k_1k_3	k_2k_3	k_1k_2	k_4	0	0
3	k_1k_4	k_2k_4	0	0	k_3k_4	$k_1k_2k_3$
4	$k_1k_3k_4$	$k_2k_3k_4$	$k_1k_2k_4$	0	0	0
5	$k_1k_2k_3k_4$	0	0	0	0	0

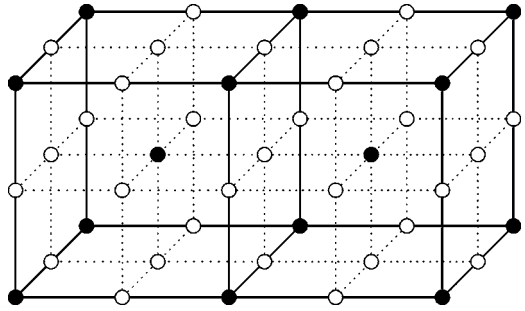

FIG. 3. Body-centered-cubic lattice (black points) obtained by applying an infinite-strength external potential at the white points of a simple cubic lattice. Hard cubes with $\sigma=2$ can only be placed at black points, thus the interaction potential becomes a nearest-neighbor exclusion in the bcc lattice.

where

$$n^{(\pm)}(\mathbf{s})=\rho(\mathbf{s})+\rho(\mathbf{s}\pm\mathbf{e}_1)+\rho(\mathbf{s}\pm\mathbf{e}_2)+\rho(\mathbf{s}\pm\mathbf{e}_3),$$

$$n^{(l)}(\mathbf{s})=\rho(\mathbf{s})+\rho(\mathbf{s}+\mathbf{e}_l),\quad l=1,\ldots,6. \tag{25}$$

The diagrammatic notation is of little help in this case, so we omit it.

E. Body-centered-cubic lattice

It is impossible to reduce a hypercubic four-dimensional lattice to a three-dimensional bcc lattice by projecting on a hyperplane. Therefore, the method used in the previous cases is not suitable for this one. But there exists a different procedure to obtain the functional for this system. Again, we will begin with a system of parallel hard cubes, but now of the same dimensionality of the target system. Also, the key ingredient of the method is to apply an infinite-strength external potential to the appropriate set of lattice sites.

Let us consider a three-dimensional system of parallel hard cubes with $\sigma=2$ in a simple cubic lattice. If we now restrict the centers of mass of the cubes to the set

$$\mathcal{L}=\{(s_1,s_2,s_3)\in\mathbb{Z}^3:\ \text{all } s_i \text{ odd or all even}\}, \tag{26}$$

then $\mathcal{L}$ forms a bcc lattice and the exclusion of the cubes in the original lattice corresponds to nearest-neighbor exclusion in the effective lattice. This transformation is sketched in Fig. 3. The effect of this external potential in the density profile of the original system amounts to

$$\rho(\mathbf{s})=\rho\left(\frac{s_2+s_3}{2},\frac{s_1+s_3}{2},\frac{s_1+s_2}{2}\right)\delta_{\mathcal{L}}(\mathbf{s}), \tag{27}$$

where $\delta_{\mathcal{L}}(\mathbf{s})=1$ if $\mathbf{s}\in\mathcal{L}$ and 0 otherwise, and the coordinates in the density profile of the rhs are referred to the basis $\{\mathbf{e}_1=\mathbf{b}_2+\mathbf{b}_3-\mathbf{b}_1,\ \mathbf{e}_2=\mathbf{b}_1+\mathbf{b}_3-\mathbf{b}_2,\ \mathbf{e}_3=\mathbf{b}_1+\mathbf{b}_2-\mathbf{b}_3\}$, $\{\mathbf{b}_1,\ \mathbf{b}_2,\ \mathbf{b}_3\}$ being the canonical vector basis in $\mathbb{Z}^3$.

In order to calculate the contribution of each weighted density $n^{(\mathbf{k})}(\mathbf{s})$ we will take into account that

$$\sum_{\mathbf{s}\in\mathbb{Z}^3}=\sum_{u=0}^{3}\ \sum_{\mathbf{s}+\mathbf{b}_u\in\mathcal{L}},$$

where $\mathbf{b}_0=(0,0,0)$. Then, after making use of the translational invariance in $\mathbf{s}$, we have for the contribution of $n^{(\mathbf{k})}(\mathbf{s})$,

$$\sum_{\mathbf{s}\in\mathcal{L}}\sum_{u=0}^{3}\Phi_0\left(\sum_{(\mathbf{r}|u,\mathbf{k})}\rho(\mathbf{s}+\mathbf{r}-\mathbf{b}_u)\right),$$

where condition $(\mathbf{r}|u,\mathbf{k})$ selects those $\mathbf{r}\in\mathcal{B}(\mathbf{k})$ such that $\mathbf{r}-\mathbf{b}_u\in\mathcal{L}$. In a more convenient way, the previous expression can be written

$$\sum_{\mathbf{s}\in\mathbb{Z}^3}\sum_{u=0}^{3}\Phi_0\left(\sum_{l=0}^{4}a_l(\mathbf{k})\rho(\mathbf{s}+\mathbf{e}_l)\right), \tag{28}$$

where $\mathbf{e}_4=\mathbf{e}_1+\mathbf{e}_2+\mathbf{e}_3$, the coefficients $a_l(\mathbf{k})$ are given in Table V, and all the spatial vectors appearing are referred to the vector basis of $\mathcal{L}$.

Taking into account the contribution of all the involved weighted densities, the total excess free-energy results

$$\beta\mathcal{F}_{\text{ex}}^{\text{bcc}}[\rho]=\sum_{\mathbf{s}\in\mathbb{Z}^3}\left[\sum_{l=1}^{4}\Phi_0(n^{(l)}(\mathbf{s}))-7\Phi_0(\rho(\mathbf{s}))\right], \tag{29}$$

with $n^{(l)}(\mathbf{s})=\rho(\mathbf{s})+\rho(\mathbf{s}+\mathbf{e}_l)$. Again, the diagrammatic notation is not much help in this case either.

III. THERMODYNAMICS

In the preceding section, we have obtained the density functional for all systems in closed form. From them it is possible to derive all the equilibrium properties of the system in the presence of an arbitrary external potential. In this section we will restrict ourselves to the bulk phase diagram. The description of bulk behavior that lattice FM functionals provide turns out to be equivalent to that obtained from other

TABLE V. The same as Table I for the linear combinations in Eq. (28) defining the weighted densities for the nearest-neighbor exclusion lattice gas in the bcc lattice.

u	$a_0(\mathbf{k})$	$a_1(\mathbf{k})$	$a_2(\mathbf{k})$	$a_3(\mathbf{k})$	$a_4(\mathbf{k})$
0	1	0	0	0	$k_1k_2k_3$
1	k_1	k_2	k_3	0	0
2	k_2	0	k_1k_3	0	0
3	k_3	0	0	k_1k_2	0

TABLE VI. Transitions of nearest-neighbor exclusion lattice gases, as predicted by FM functionals.

Lattice	Order	η	βp	z	$-\Phi$
Square	second	1/2	0.523	1.687	0.392
triangular	first	0.684-0.754	0.737	7.70	—
sc	second	1/3	0.305	0.763	0.350
fcc	first	0.579-0.837	0.461	5.29	—
bcc	second	1/4	0.216	0.490	0.305

classical theories. Thus in this particular application it provides nothing new, and we include it both for completeness and to show the remarkable fact that FM theory subsumes many other theories in a unified framework. Anyhow, we want to stress that what FM theory provides are functionals, and functionals perform best when applied to inhomogeneous problems. The phase transitions obtained for each model are collected in Table VI.

A. Square lattice

As the interaction is only between nearest neighbors, we will distinguish two sublattices in such a way that the nearest neighbors of every site of one sublattice belong to the other sublattice. Let the density of each sublattice be ρ_1 and ρ_2. Given a total density ρ it holds $2\rho=\rho_1+\rho_2$. When we consider such a density profile in Eq. (7) the free-energy density becomes

$$\Phi^{\mathrm{sq}}=\Phi_{\mathrm{id}}+2\Phi_0(\eta)-\tfrac{3}{2}[\Phi_0(\rho_1)+\Phi_0(\eta-\rho_1)], \quad (30)$$

where $0\leqslant\eta=2\rho\leqslant 1$ is the packing fraction, $\Phi_{\mathrm{id}}=(1/2)\Sigma_i\rho_i(\ln\rho_i-1)$ is the ideal contribution (recall that we are considering two lattice sites, hence the factor 1/2), and we have written $\rho_2=\eta-\rho_1$.

The equilibrium state of the system at constant packing fraction η is given by the global minimum of Eq. (30) with respect to ρ_1. This is a solution to the Euler-Lagrange equation

$$\rho_1(1-\rho_1)^3=(\eta-\rho_1)(1-\eta+\rho_1)^3. \quad (31)$$

For low values of η this state corresponds to the uniform or disordered one, with $\rho_1=\rho_2=\rho$. For higher values, one expects the system to undergo a phase transition to an ordered phase, where one of the sublattices is preferentially occupied. This situation is exactly the one described by the solutions of Eq. (31). For $0\leqslant\eta\leqslant\eta_c^{\mathrm{sq}}=1/2$ the minimum is given by $\rho_1=\rho$. The equation of state and fugacity of the disordered phase can be easily obtained from Eq. (30),

$$\beta p^{\mathrm{sq}}_{\mathrm{fluid}}=\ln\frac{(1-\eta/2)^3}{(1-\eta)^2}, \quad z^{\mathrm{sq}}_{\mathrm{fluid}}=\frac{\eta(1-\eta/2)^3}{2(1-\eta)^4}. \quad (32)$$

For $1/2\leqslant\eta\leqslant 1$, we have

$$\rho_1^{\mathrm{eq}}=\frac{1}{2}\left[\eta+(2-\eta)\sqrt{\frac{2\eta-1}{3-2\eta}}\right]. \quad (33)$$

This gives the ordered state. The equation of state and fugacity in this phase are given by

$$\beta p^{\mathrm{sq}}_{\mathrm{solid}}=\beta p^{\mathrm{sq}}_{\mathrm{fluid}}-\frac{3}{2}\ln\frac{3-2\eta}{4(1-\eta)}, \quad z^{\mathrm{sq}}_{\mathrm{solid}}=\frac{\rho_1^{\mathrm{eq}}(1-\rho_1^{\mathrm{eq}})^3}{(1-\eta)^4}. \quad (34)$$

The equation of state of both phases is plotted in Fig. 4. Also, the occupancy of each sublattice is plotted in Fig. 5. The transition is second order, and the critical point values are listed in Table VI. These are the same as those obtained by Burley [23] and Temperley [24] with a Bethe approxima-

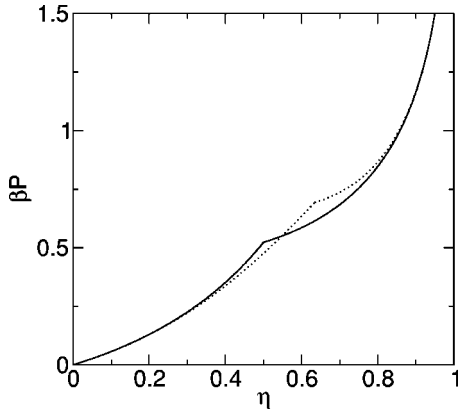

FIG. 4. Phase diagram (pressure vs packing fraction) of the hard-square lattice gas in the lattice FM approximation (solid line). The system undergoes a second-order phase transition from a disordered state to an ordered one at $\eta_c^{\mathrm{sq}}=1/2$. Dotted line: results of the ''ring'' approximation obtained by Burley [23].

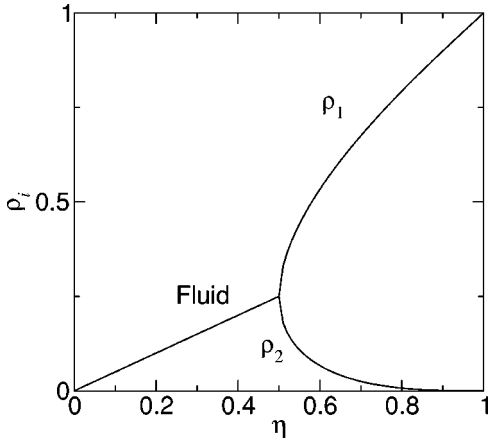

FIG. 5. Densities of the two sublattices, ρ_1 and ρ_2, for the hard-square lattice gas, as a function of the packing fraction η.

tion. The next correction to the Bethe approximation (called the ''ring'' approximation) in the scheme proposed by Rushbrooke and Scoins [25,26] has also been considered by Burley [23]. The results are plotted in Fig. 4 for comparison. The qualitative phase behavior is the same, but the critical values improve those of the Bethe approximation. A further correction (''necklace'' approximation) within the same scheme has been implemented by Temperley [27], who claims that the transition becomes first order.

B. Triangular lattice

As a triangular lattice has three sublattices such that a nearest neighbor of a site in one sublattice belongs to another sublattice, we will characterize the density profile with the densities of each sublattice: ρ_1, ρ_2, and ρ_3, the total density of the system being related to them through $3\rho=\rho_1+\rho_2+\rho_3$.

The free-energy density for a three sublattice configuration can be obtained from Eq. (13)

$$\Phi^{\mathrm{tr}}=\Phi_{\mathrm{id}}+2\Phi_0(\eta)-\Phi_0(\rho_1+\rho_2)-\Phi_0(\rho_1+\rho_3)-\Phi_0(\rho_2+\rho_3)+\tfrac{1}{3}[\Phi_0(\rho_1)+\Phi_0(\rho_2)+\Phi_0(\rho_3)], \tag{35}$$

where $0\leqslant\eta=3\rho\leqslant 1$ and $\Phi_{\mathrm{id}}=(1/3)\Sigma_i\rho_i(\ln\rho_i-1)$. As in the previous case, the phase diagram can be obtained by minimizing this free-energy density at constant packing fraction. For low values of the density the stable phase is uniform, so $\rho_1=\rho_2=\rho_3=\rho$. In contrast, for high values of the density one sublattice is preferentially occupied. In this ordered phase the configuration that results from Eq. (35) is $\rho_1\geqslant\rho_2=\rho_3$. Thus, in what follows we will consider the latter two sublattices as equivalent. The Euler-Lagrange equation obtained from Eq. (35) is

$$\frac{\rho_2(1-2\rho_2)^3(1-\eta+2\rho_2)}{(1-\rho_2)(\eta-2\rho_2)(1-\eta+\rho_2)^3}=1. \tag{36}$$

The solutions to this equation as a function of η indicate a first-order transition. The coexisting packing fractions as well as the pressure and fugacity at coexistence appear in Table VI. The equation of state for the disordered phase is

$$\beta p^{\mathrm{tr}}_{\mathrm{fluid}}=\ln\frac{(1-2\eta/3)^3}{(1-\eta/3)(1-\eta)^2}, \tag{37}$$

and the fugacity

$$z^{\mathrm{tr}}_{\mathrm{fluid}}=\frac{\eta(1-2\eta/3)^6}{3(1-\eta/3)(1-\eta)^6}. \tag{38}$$

For the ordered phase

$$\beta p^{\mathrm{tr}}_{\mathrm{solid}}=\frac{1}{3}\ln\frac{(1-\eta+\rho_2)^6(1-2\rho_2)^3}{(1-\eta)^6(1-\eta+2\rho_2)(1-\rho_2)^2}, \tag{39}$$

and

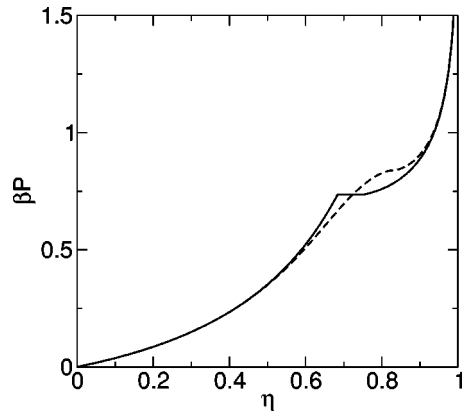

FIG. 6. The same as Fig. 4 for the hard-hexagon model (nearest-neighbor exclusion in a triangular lattice). Solid line represents the equation of state from the FM approximation. Dashed line represents the exact solution by Baxter [28]. In our approach the system undergoes a first-order phase transition from a disordered phase to an ordered one. Coexisting packing fractions are $\eta_{\mathrm{fluid}}=0.684$ and $\eta_{\mathrm{solid}}=0.754$. It is worth mentioning the good agreement of FM approximation with the exact solution at low and high densities, despite its failure in the critical region.

$$z^{\mathrm{tr}}_{\mathrm{solid}}=\frac{\rho_2(1-\eta+\rho_2)^3(1-2\rho_2)^3}{(1-\eta)^6(1-\rho_2)}, \tag{40}$$

where ρ_2 is given by Eq. (36). The phase diagram is plotted in Fig. 6. Sublattice densities are shown in Fig. 7.

This result coincides with that obtained by Burley [29] by using the ring approximation (see Sec. III A), and was also obtained by Temperley through a combinatorial finite matrix method [24].

This system has been exactly solved by Baxter [28,30]. This fact allows us to compare not only the equation of state (Fig. 6) and sublattice occupancy (Fig. 7), but also the compressibility (Fig. 8). The system exhibits a *continuous* phase transition (the critical point in the pressure vs density diagram is a horizontal inflection point) at packing fraction $\eta_c^{\mathrm{exact}}=(3/10)(5-\sqrt{5})\approx 0.829$ and critical pressure $\beta p_c^{\mathrm{exact}}$

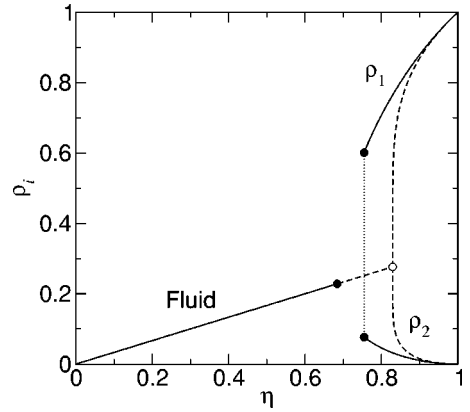

FIG. 7. The same as Fig. 5 for the triangular lattice. Full circles represent the configuration of coexisting phases. Dashed lines are sublattice densities in the exact solution. The empty circle is the exact critical point.

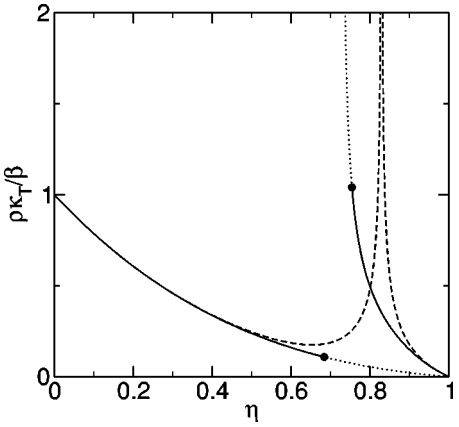

FIG. 8. Reduced compressibility ($\rho\kappa_T/\beta$) vs the packing fraction (η) for the triangular lattice. Full circles denote the coexisting points. Dotted lines extrapolate the compressibility in the metastable region. (The extrapolation for the fluid line actually breaks down at around $\eta\approx 0.88$, because the entropy becomes negative beyond that point.) Baxter's exact solution is represented with dashed lines.

$=(1/2)\ln[(27/250)(25+11\sqrt{5})]\approx 0.839$. To the best of our knowledge, this is the first time that FM theory can be compared with an exact result in a dimension higher than one. Although the theory fails in predicting correctly the order of the transition, the agreement in the whole range of density except the critical region is rather accurate.

C. Simple cubic lattice

In the close-packed state the particles of this system occupy one sublattice with fcc symmetry, while the sublattice formed by nearest neighbors of that one remains empty. Thus, we will only consider these two sublattices, with densities ρ_1 and ρ_2, respectively. Again, the total density ρ is related to these numbers by $2\rho=\rho_1+\rho_2$.

When we insert such a density profile in the functional (19) we get for the free-energy density

$$\Phi^{\rm sc}=\Phi_{\rm id}+\Phi_0(2\rho)-\tfrac{5}{2}[\Phi_0(\rho_1)+\Phi_0(2\rho-\rho_1)], \quad (41)$$

where we have eliminated the dependency on ρ_2. For a fixed value of the density, the global minimum of Eq. (41) is a solution to the Euler-Lagrange equation

$$\frac{\rho_1(1-\rho_1)^5}{(\eta-\rho_1)(1-\eta+\rho_1)^5}=1, \quad (42)$$

$0\leqslant\eta=2\rho\leqslant 1$ being the packing fraction. When $0\leqslant\eta\leqslant\eta_c^{\rm sc}=1/3$, the minimum is given by the uniform phase $\rho_1^{\rm eq}=\eta$. For the equation of state and fugacity we have

$$\beta p^{\rm sc}_{\rm fluid}=\ln\frac{(1-\eta/2)^5}{(1-\eta)^3}, \quad z^{\rm sc}_{\rm fluid}=\frac{\eta(1-\eta/2)^5}{2(1-\eta)^6}. \quad (43)$$

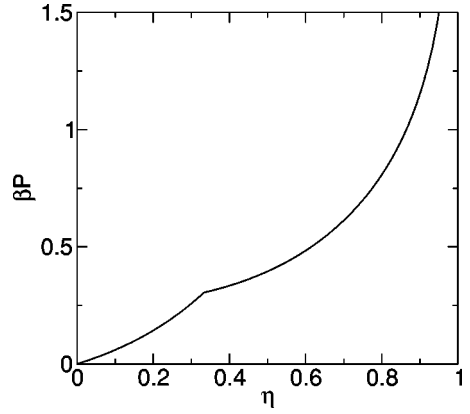

FIG. 9. The same as Fig. 4 for the nearest-neighbor exclusion lattice gas in the simple cubic lattice. A second-order transition is predicted at $\eta_c^{\rm sc}=1/3$.

Upon increasing the density the system experiences a second-order disorder-order transition at $\eta_c^{\rm sc}=1/3$. For $1/3\leqslant\eta\leqslant 1$, the density of the preferred sublattice can be calculated from Eq. (42) to be

$$\rho_1^{\rm eq}=\frac{1}{2}\left\{\eta+(2-\eta)\sqrt{\frac{2[5-4\eta(2-\eta)]^{1/2}-5(1-\eta)}{5-3\eta}}\right\}. \quad (44)$$

In this phase, the equation of state is given by

$$\beta p^{\rm sc}_{\rm solid}=\beta p^{\rm sc}_{\rm fluid}+\frac{5}{2}\ln\left[\frac{2(5-4\eta)-\sqrt{5-4\eta(2-\eta)}}{5-3\eta}\right], \quad (45)$$

and the fugacity by

$$z^{\rm sc}_{\rm solid}=\frac{\rho_1^{\rm eq}(1-\rho_1^{\rm eq})^5}{(1-\eta)^6}. \quad (46)$$

The equation of state is plotted in Fig. 9. Sublattice densities are shown in Fig. 10. The critical point values are listed in Table VI. As for the square lattice, for this model the result from FM theory coincides with a Bethe approximation [23].

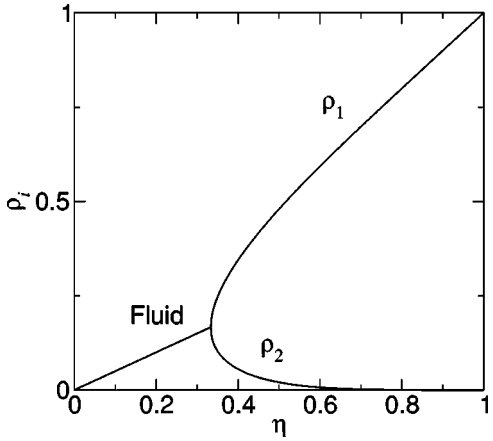

FIG. 10. The same as Fig. 5 for the simple cubic lattice.

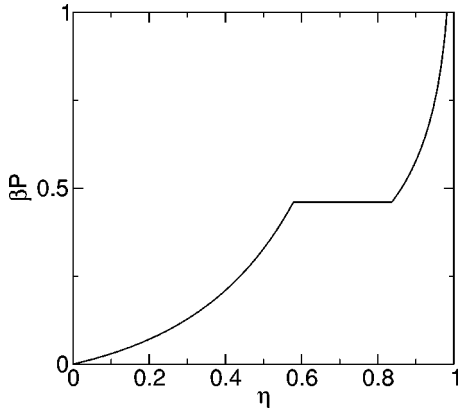

FIG. 11. The same as Fig. 4 for the nearest-neighbor exclusion in the face-centered-cubic lattice. A first-order phase transition takes place at pressure $\beta p = 0.461$ with coexisting states at $\eta_{\text{fluid}}^{\text{fcc}} = 0.579$ and $\eta_{\text{solid}}^{\text{fcc}} = 0.837$.

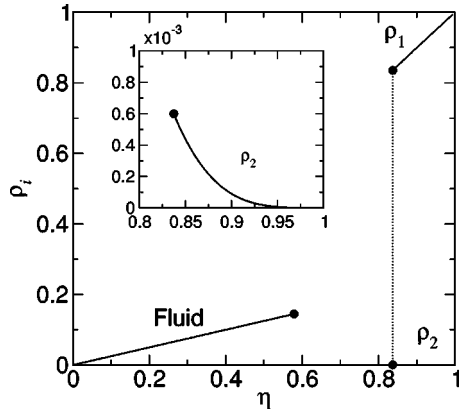

FIG. 12. The same as Fig. 5 for the fcc lattice. Solid circles represent configurations of coexisting phases. The inset shows a detail of sublattice density ρ_2.

As far as we know, the only available simulation data are the critical exponents (which we cannot compare with since a Bethe approximation is mean field) and the critical fugacity $z_c = 1.0559$ [31,32]. The agreement with the predicted value (shown in Table VI) is poor, but z_c is certainly not the best output one should expect from a Bethe approximation. Unfortunately, no other magnitudes have been simulated to make a more fair comparison.

D. Face-centered-cubic lattice

A fcc lattice contains four equivalent sublattices each with a sc symmetry. As in the previous cases sublattice densities are denoted, ρ_1, ρ_2, ρ_3, ρ_4, and $\eta = 4\rho = \rho_1 + \rho_2 + \rho_3 + \rho_4$ holds for the total density ρ or packing fraction η.

The free-energy density for such a density profile in the FM approximation is obtained from Eq. (24) as

$$\Phi^{\text{fcc}} = \Phi_{\text{id}} + 2\Phi_0(\eta) - \sum_{i<j} \Phi_0(\rho_i + \rho_j) + \frac{5}{4}\sum_{i=1}^{4} \Phi_0(\rho_i), \tag{47}$$

where $\Phi_{\text{id}} = (1/4)\Sigma_i \rho_i(\ln \rho_i - 1)$. The global minimum of Φ_{fcc} at fixed density with respect to the sublattice densities yields the thermodynamically stable phase. But now there is a subtle point we have to take into account: the close packing is degenerated. If we consider the fcc lattice as a stacking of square lattices each having its sites on the centers of the squares of the previous one, then we can fill alternative layers independently. Thus, we will consider different densities for the four sublattices and the minimum of the free energy will determine the structure of the most stable phase. (Previous studies [33] impose the equivalence of three sublattices from the beginning, i.e., $\rho_1 \neq \rho_2 = \rho_3 = \rho_4$.)

Solving numerically the Euler-Lagrange equations obtained from Eq. (47) at fixed packing fraction, we obtain the equation of state plotted in Fig. 11. Sublattice densities at equilibrium phases are shown in Fig. 12. The system undergoes a first-order phase transition to an ordered phase with $\rho_1 \neq \rho_2 = \rho_3 = \rho_4$. (See Table VI for the critical point values.) For the uniform phase

$$\beta p_{\text{fluid}}^{\text{fcc}} = \ln \frac{(1-\eta/2)^6}{(1-\eta/4)^5(1-\eta)^2} \tag{48}$$

and

$$z_{\text{fluid}}^{\text{fcc}} = \frac{\eta(1-\eta/2)^{12}}{4(1-\eta/4)^5(1-\eta)^8}. \tag{49}$$

For the ordered phase

$$\beta p_{\text{solid}}^{\text{fcc}} = \frac{1}{4}\ln \frac{(1-\eta+2\rho_2)^{12}(1-2\rho_2)^{12}}{(1-\eta+3\rho_2)^5(1-\rho_2)^{15}(1-\eta)^8} \tag{50}$$

and

$$z_{\text{solid}}^{\text{fcc}} = \frac{\rho_2(1-\eta+2\rho_2)^4(1-2\rho_2)^8}{(1-\rho_2)^5(1-\eta)^8}, \tag{51}$$

with ρ_2 the minimum of the free energy (47).

It is worth mentioning that a metastable phase transition from the disordered state to a smectic ordered state (alternative square-lattice layers are uniformly occupied, with densities ρ_1 and ρ_2) is also obtained from the functional (47).

E. Body-centered-cubic

At a close-packing state this system has one sublattice completely filled while the nearest-neighbor sublattice is empty. Therefore, we will consider the density profile as in the previous similar cases (square or sc lattices).

The free-energy density [Eq. (29)] becomes

$$\Phi^{\text{bcc}} = \Phi_{\text{id}} + 4\Phi_0(\eta) - \tfrac{7}{2}[\Phi_0(\rho_1) + \Phi_0(\eta - \rho_1)]. \tag{52}$$

The Euler-Lagrange equation is

$$\frac{\rho_1(1-\rho_1)^7}{(\eta-\rho_1)(1-\eta+\rho_1)^7} = 1. \tag{53}$$

The phase behavior obtained from this equation is similar to that of the square or the sc lattices: The system undergoes a second-order phase transition at $\eta_c^{\text{bcc}} = 1/4$; below this den-

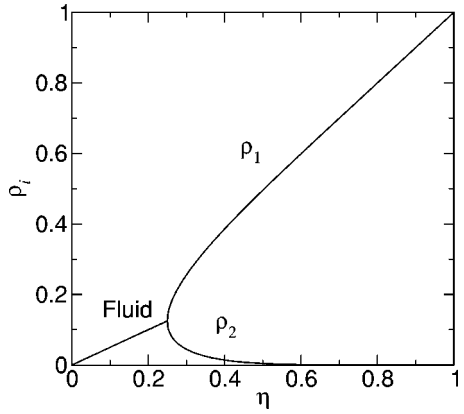

FIG. 13. The same as Fig. 5 for the bcc lattice.

sity the stable phase is a fluid, while above the particles occupy preferentially one sublattice. The ordered solution of Eq. (53) can be obtained analytically, but the expression is rather cumbersome, so we just plot it in Fig. 13. For the fluid phase, the equation of state and fugacity are given by

$$\beta p_{\rm fluid}^{\rm bcc} = \ln \frac{(1-\eta/2)^7}{(1-\eta)^4}, \quad z_{\rm fluid}^{\rm bcc} = \frac{\eta(1-\eta/2)^7}{2(1-\eta)^8}. \tag{54}$$

For the ordered phase, we have

$$\beta p_{\rm solid}^{\rm bcc} = \frac{1}{2} \ln \frac{(1-\rho_1)^7(1-\eta+\rho_1)^7}{(1-\eta)^4}, \tag{55}$$

and

$$z_{\rm solid}^{\rm bcc} = \frac{\rho_1(1-\rho_1)^7}{(1-\eta)^8}, \tag{56}$$

with ρ_1 the ordered solution of Eq. (53).

These results are again equivalent to those obtained with a Bethe approximation [23]. The equation of state is plotted in Fig. 14 (see Table VI for the critical point values).

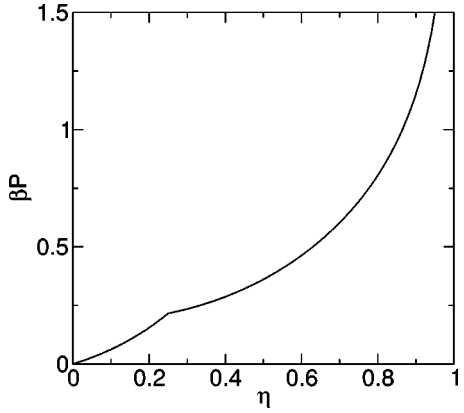

FIG. 14. The same as Fig. 4 for the nearest-neighbor exclusion lattice gas in the bcc lattice. The system undergoes a second-order phase ordering transition at $\eta_c^{\rm bcc} = 1/4$.

As for the sc lattice, the only available simulation data to compare with is the critical fugacity $z_c = 0.7223$ [34]. Again and for a similar reason, it compares poorly with the value listed in Table VI.

IV. DISCUSSIONS AND CONCLUSIONS

Dimensional crossover is a property that connects different models. A system of parallel hard cubes (both on and off a lattice) constrained to lie on a plane parallel to their sides becomes a system of parallel hard squares. A system of parallel hard squares constrained to lie on a straight line parallel to their edges becomes a system of hard rods. These are obvious dimensional crossovers, but in this paper we have introduced a few more: parallel hard cubes constrained to lie on more general planes produce nearest-neighbor exclusion lattice gases in the square and triangular lattices; four-dimensional parallel hard hypercubes constrained to lie on certain hyperplanes become nearest-neighbor exclusion lattice gases in the sc or fcc lattices. If this dimensional constraint is regarded as the application of an infinite-strength external field, then more general patterns of such an external field produce new models out of the parallel hard cube one (the nearest-neighbor exclusion lattice gas in the bcc lattice, for instance).

The message we want to transmit with this work is that FM functionals for all these models have the remarkable property of being connected with each other through the same transformations. More than that: further dimensional crossovers of these models are also consistently captured by FM functionals. For instance, all functionals obtained in this paper produce the *exact* functional for hard rods when reduced to one dimension; also, the functional for the nearest-neighbor lattice gas in the square lattice, Eq. (7), can be obtained from the one in either the sc lattice, Eq. (19), the fcc lattice, Eq. (24), or the bcc lattice, Eq. (29), through the application of an appropriate external potential. Similarly, the functional for the nearest-neighbor lattice gas in the triangular lattice, Eq. (13), can be recovered from that in the fcc lattice, Eq. (24). Such a degree of internal consistency is not shared by any other known density functional theory, and it puts FM theory at a different level. As a byproduct, as pointed out in the Introduction, it warrants a good behavior of FM functionals when dealing with highly inhomogeneous situations.

When applied to study the bulk phase behavior of these nearest-neighbor lattice gases, FM functionals produce reasonable results, sometimes with important discrepancies in the critical region, sometimes more accurate, and always very accurate at low and high densities. There are, no doubt, better methods to fit the equation of state and obtain a better description of this phase behavior, such as, for instance, finite-size analysis [35–38] or series expansions [33,37,39,40]. They are particularly useful in predicting the critical behavior. The FM approach has an important advantage on these methods, whatever the sacrifice in accuracy: it leads to simple, closed-form functionals. Thus it permits us to study inhomogeneous problems, which are absolutely out of the scope of these other more accurate methods. A particu-

larly interesting example of such inhomogeneous problems can be found in recent studies of fluids in porous media [19–21], for which lattice models seem to capture enough physical information to describe many interesting phenomena not yet described by other models.

An interesting observation to make from the results of the application of the FM theory to describe bulk phase behavior is the close connection it has with other classical approaches. For those lattices with only two sublattices (loose-packed lattices) FM theory reduces to a Bethe approximation (square, sc, and bcc lattices); for lattices with more than one sublattice (close-packed lattices) it becomes equivalent to another clusterlike approximation. In fact, when closely looked at, all these approximation are but particular cases of Kikuchi's cluster variation theory [41]. This theory proposes a hierarchical scheme of approximations under the basis of describing in an exact manner clusters of increasing size. Roughly speaking, the larger the cluster the more accurate the results—and the more involved the theory. The connection between FM theory and the cluster variation method is definitely worth exploring, because one drawback of the latter is that there is not an *a priori* criterion to choose the clusters, other than ''the larger the better;'' as a matter of fact, some clusters (depending on the model) produce an optimal result and some others (even larger ones) spoil the accuracy, and the reason for that is unknown. FM theory, on the contrary, leaves no freedom to choose the clusters, but those it prescribes seem to be optimal in the above sense. Burley's treatment of the nearest-neighbor exclusion lattice gas in the fcc lattice is very illustrative [23]: the inappropriate election of the clusters [only part of those prescribed by the FM functional (24)] leads to a spurious divergence of the free energy at a density lower than the close packing. This is a line of investigation we are currently following.

ACKNOWLEDGMENTS

This work was supported by Project No. BFM2000-0004 of the Dirección General de Investigación (DGI) of the Spanish Ministerio de Ciencia y Tecnología.

[1] Y. Rosenfeld, Phys. Rev. Lett. **63**, 980 (1989).
[2] P. Tarazona and Y. Rosenfeld, Phys. Rev. E **55**, R4873 (1997).
[3] P. Tarazona, Phys. Rev. Lett. **84**, 694 (2000).
[4] J. A. Cuesta, Y. Martínez-Ratón, and P. Tarazona, J. Phys.: Condens. Matter **14**, 11965 (2002).
[5] Y. Rosenfeld and P. Tarazona, Mol. Phys. **95**, 141 (1998).
[6] P. Tarazona, Physica A **306**, 243 (2002).
[7] R. Roth, R. Evans, A. Lang, and G. Kahl, J. Phys.: Condens. Matter **14**, 12063 (2002).
[8] Y. Rosenfeld, M. Schmidt, H. Löwen, and P. Tarazona, J. Phys.: Condens. Matter **8**, L577 (1996).
[9] Y. Rosenfeld, M. Schmidt, H. Löwen, and P. Tarazona, Phys. Rev. E **55**, 4245 (1997).
[10] J. A. Cuesta and Y. Martínez-Ratón, Phys. Rev. Lett. **78**, 3681 (1997).
[11] M. Schmidt, Phys. Rev. E **60**, R6291 (1999).
[12] M. Schmidt and C. von Ferber, Phys. Rev. E **64**, 051115 (2001).
[13] J. M. Brader, A. Esztermann, and M. Schmidt, Phys. Rev. E **66**, 031401 (2002).
[14] M. Schmidt and A. R. Denton, Phys. Rev. E **65**, 061410 (2002).
[15] L. Lafuente and J. A. Cuesta, Phys. Rev. Lett. **89**, 145701 (2002).
[16] L. Lafuente and J. A. Cuesta, J. Phys.: Condens. Matter **14**, 12079 (2002).
[17] L. Lafuente and J. A. Cuesta, J. Chem. Phys. **119**, 10832 (2003).
[18] M. Schmidt, Phys. Rev. E **66**, 041108 (2002).
[19] M. Schmidt, L. Lafuente, and J. A. Cuesta, J. Phys.: Condens. Matter **15**, 4695 (2003).
[20] E. Kierlik, P. A. Monson, M. L. Rosinberg, L. Sarkisov, and G. Tarjus, Phys. Rev. Lett. **87**, 055701 (2001).
[21] E. Kierlik, P. A. Monson, M. L. Rosinberg, and G. Tarjus, J. Phys.: Condens. Matter **14**, 9295 (2002).
[22] L. K. Runnels, in *Phase Transitions and Critical Phenomena*, edited by C. Domb and M. S. Green (Academic Press, London, 1972), Vol. 2, Chap. 8, pp. 305–328.
[23] D. M. Burley, Proc. Phys. Soc. **77**, 451 (1961).
[24] H. N. V. Temperley, Proc. Phys. Soc. **77**, 630 (1961).
[25] G. S. Rushbrooke and H. I. Scoins, Proc. R. Soc. London, Ser. A **230**, 74 (1955).
[26] H. N. V. Temperley, Proc. Phys. Soc. **80**, 813 (1962).
[27] H. N. V. Temperley, Proc. Phys. Soc. **80**, 823 (1962).
[28] R. J. Baxter, *Exactly Solved Models in Statistical Mechanics* (Academic Press, London, 1982).
[29] D. M. Burley, Proc. Phys. Soc. London **85**, 1173 (1965).
[30] R. J. Baxter, J. Phys. A **13**, L61 (1980).
[31] J. R. Heringa and H. W. J. Blöte, Physica A **232**, 369 (1996).
[32] A. Yamagata, Physica A **215**, 511 (1995).
[33] D. S. Gaunt, J. Chem. Phys. **46**, 3237 (1967).
[34] A. Yamagata, Physica A **231**, 495 (1996).
[35] L. K. Runnels, Phys. Rev. Lett. **15**, 581 (1965).
[36] F. H. Ree and D. A. Chesnut, J. Chem. Phys. **45**, 3983 (1966).
[37] J. Orban and A. Bellemans, J. Chem. Phys. **49**, 363 (1968).
[38] W. Guo and H. W. J. Blöte, Phys. Rev. E **66**, 046140 (2002).
[39] D. S. Gaunt and M. E. Fisher, J. Chem. Phys. **43**, 2840 (1965).
[40] R. J. Baxter, I. G. Enting, and K. Tsang, J. Stat. Phys. **22**, 465 (1980).
[41] R. Kikuchi, Phys. Rev. **81**, 988 (1951).
[42] J. K. Percus, J. Stat. Phys. **15**, 505 (1976).
[43] P. Tarazona (private communication).